



22 **1. Introduction**

23 Efficient development and optimum utilization of water resources is of great significance to the
24 overall development of any country. Many rivers, springs and lakes in the mountain regions are
25 fed by the significant contribution of runoff from the snow melt and glacier melt. High spatial and
26 temporal variability in hydro-metrological conditions in mountainous environments requires
27 spatial models that are physically realistic and computationally efficient (Liston et al. 2006).

28 Hydrological ecosystem services (ES) often include drinking waters supply, power production,
29 industrial use, irrigation, and many more. These hydrological ES are dependent on the
30 characteristics of different watersheds such a topography, land use land cover (LULC), soil type
31 and its climatic condition.

32 To quantify the impact of land-use and land management decisions on ecosystem services, a
33 number of tools have been developed by various researchers (Bagstad et al. 2013). Accordingly,
34 models for ecosystem-service valuation often focus on using globally available data, accepting
35 large number of spatially explicit inputs and producing spatially explicit output, and limiting the
36 model structure to key biophysical processes involved in land-use change (Guswa et al. 2014).

37 Due to the spatial variability and dependency on so many topographical and climatic factors, the
38 proper analysis of ES happens to be a complicated task. The benefits that can be derived from ES
39 should be analyzed and quantified in a spatially explicit manner (Sanchez et al. 2012). The
40 uncertainties in the determination of spatial and temporal distribution of the climatic variables,
41 especially precipitation constitutes a major obstacle to the understanding of hydrological behavior
42 at the catchment scales (Milly et al. 2002).



43 The literature indicates attempts to develop different ecosystem assessment tools. In this respect,
44 Integrated Valuation of Ecosystem Services and Tradeoffs (InVEST), developed by Natural
45 Capital Project (Tallis et al. 2010) is worth mention. It includes a biophysical component,
46 computing the provision of freshwater or water yield, by different parts of the landscape and a
47 valuation component, representing the benefits of water provisioning to people. This model is very
48 simplified and is based upon the Budyko theory, which has a long history and still continues to
49 receive interest in the hydrological literature (Budyko 1979; Zhou et al. 2012; Zhang et al. 2004;
50 Ojha et al. 2008; Zhang et al. 2001; Donohue et al. 2012; Xu et al. 2013; Wang et al. 2014). The
51 InVEST model applies a one-parameter formulation of the theory in a semi-distributed way (Zhang
52 et al. 2004).

53 In literature, some of the limitations related to InVEST annual water yield model, are that there is
54 an absence or inadequate comparison with observed data, calibration of the model without prior
55 identification of sensitive parameters, and lack of validation of the predictive capabilities in the
56 context of Land Use Land Cover change (Bai et al. 2012; Nelson et al. 2010; Su et al. 2013; Terrado
57 et al. 2014).

58 In 2012, the sensitivity analysis is done by Sanchez-Canales *et al.* using the InVEST model for a
59 Mediterranean region basin for three parameters i.e. Z (seasonal precipitation coefficient),
60 precipitation (annual) and ET_0 (annual reference precipitation) and found that precipitation as the
61 most sensitive parameter. Later in 2014, Terrado et al., applied the InVEST model for the heavily
62 humanized Llobregat river basin. The model is applied for both extreme wet and dry conditions
63 and the role of climatic parameters is emphasized. Hoyer et al. (2014), applied this model in
64 Tualatin and Yamhill basins of northwestern Oregon under the series of urbanization and climate
65 change scenarios. The results show that the climatic parameters have more sensitivity than other



66 inputs for a water yield model. Hamel et al. (2014), applied the same water yield model for the
67 Cape Fear catchment, North Carolina and concluded that the precipitation is the most influencing
68 parameter. Goyal et al. (2017) analyzed the InVEST water yield model for the hilly catchment by
69 taking two catchments i.e. Sutlej river catchment and Tungabhadra river catchment. The climate
70 parameters i.e. precipitation and ET_0 are observed to be most influencing parameters. However,
71 spatial variability of some of the model parameters is not accounted for in this work.

72 This work primarily considers in detail, the spatial variation of used model parameters and uses
73 different strategies to compute water yield. Such water yield estimates are computed for four years
74 i.e. 1980, 1990, 2001 and 2015 to identify most successful strategy. The parameters that are earlier
75 computed at basins level scale are reduced to pixel level scale in order to study hydrological
76 processes of catchment at pixel level to increase the efficiency of the results.

77 **2. Background Theory**

78 ***2.1 Water Yield Models***

79 In this section, two water yield models, i.e. InVEST water yield model, which is a distributed
80 model and Lumped Zhang model is described as follows.

81 ***2.1.1 InVEST model***

82 The InVEST water yield model (Tallis *et al.* 2010) is designed to provide the information regarding
83 the changes in the ecosystem that are likely to alter the flows. It is based upon the Budyko theory
84 which is an empirical function that yields the ratio of actual to potential evapotranspiration
85 (Budyko, 1979). To describe the degree to which long-term catchment water-balances deviate
86 from the theoretical limits, a number of scholars have proposed one-parameter functions that can
87 replicate the Budyko curve (Fu 1981, Choudhury 1999, Zhang et al. 2004, Wang et al. 2014)



88 To observe and represent parcel-level changes to the landscape, InVEST model represents
89 explicitly the spatial variability in precipitation and PET, soil depth and vegetation. The model
90 runs in the gridded format and acquires the inputs in the raster format which in turn helps to
91 understand the heterogeneity of the factors influencing the water yield such as precipitation, land
92 use land cover, soil type, etc. GIS and remote sensing plays a very crucial role in gathering the
93 spatial and temporal information of any hydrological processes. GIS could be utilized as a suitable
94 tool for solving water resources problems from local to global scale, spatially as well as temporally
95 (Khatami et al. 2014).

96 The water yield model is based on an empirical function which is known as the Budyko curve
97 (Budyko 1974). The model takes the input as raster format and runs on the gridded map. Water
98 yield $Y(x)$ is determined for each pixel annually on a landscape as follows:

$$99 \quad Y(x) = \left(1 - \frac{AET(x)}{P(x)}\right) \times P(x) \quad (1)$$

100 Where, $AET(x)$ is the actual annual evapotranspiration per pixel x ; and $P(x)$ is the annual
101 precipitation per pixel x .

102 Mean annual evapotranspiration of any catchment is strongly determined by precipitation and
103 potential evapotranspiration. The secondary role is played by the catchment characteristics, i.e.
104 soil, topography, etc.

105 The InVEST model uses an expression of the Budyko curve by Fu (1981) and Zhang *et al.* (2004).
106 The ratio of mean annual potential evapotranspiration to annual precipitation, known as index of
107 dryness, can be used to determine the mean annual evapotranspiration by using one additional
108 parameter.



$$109 \quad \frac{AET(x)}{P(x)} = 1 + \frac{PET(x)}{P(x)} - \left[1 + \frac{PET(x)}{P(x)} \right]^{\left(\frac{1}{\omega}\right)} \quad (2)$$

110 Where, $PET(x)$ is the annual potential evapotranspiration per pixel x (mm); and $\omega(x)$ is a non-
 111 physical parameter that influences the natural climatic soil properties.

112 The $PET(x)$ is calculated by the following expression:

$$113 \quad PET(x) = Kc(x) \times ET_o(x) \quad (3)$$

114 Where, $ET_o(x)$ is the annual reference evapotranspiration per pixel x which is calculated based
 115 on evapotranspiration of grass of alfalfa grown at that location shown in the equation (6). $Kc(x)$
 116 is the vegetation evapotranspiration coefficient that is influenced by the change in characteristics
 117 of land use land cover for every pixel (Allen et al. 1998). The values of $ET_o(x)$ are adjusted by
 118 $Kc(x)$ for each pixel over the land use land cover map. $\omega(x)$ is an empirical parameter and the
 119 expression given by Donohue et al. (2012) for the InVEST model has been applied to define $\omega(x)$
 120 which is as follows:

$$121 \quad \omega(x) = z \times \frac{AWC(x)}{P(x)} + 1.25 \quad (4)$$

122 Thus, the minimum value of the parameter $\omega(x)$ is 1.25 for bare soil where root depth is zero
 123 (Donohue et al. 2012) which is evident from the above expression. Other parameter z is known as
 124 seasonality factor whose values vary from 1 to 30. It represents the nature of local precipitation
 125 and other hydrogeological parameters. The parameter $AWC(x)$ depicts volumetric plant available
 126 water content which is expressed in depth (mm) which can be expressed by following formula for
 127 each pixel x :

$$128 \quad AWC(x) = Min.(\text{Restricting layer depth, root depth}) \times PAWC \quad (5)$$



129 Root restricting layer depth is defined as the depth of the soil upto which the soil can allow the
130 penetration of roots and root depth is defined as the depth where 95 percent of the root biomass
131 occurs. Plant Available Water Content (PAWC) is generally taken as the difference between the
132 field capacity and wilting point. It depends upon the soil properties and can be computed by the
133 Soil-Plant-Air-Water (SPAW) software. PAWC is calculated using the method described by
134 Mckenzie et al. (2003).

135 For computing the pixel wise reference evapotranspiration for the study area, two methods are
136 applied, i.e. modified Hargreaves method and Hargreaves method.

137 Modified Hargreaves method

$$138 \quad ET_o = 0.0013 \times 0.408 \times RA \times (T_{avg} + 17.0) \times (TD - 0.0123 \times P)^{0.76} \quad (6)$$

139 Where, ET_o is reference evapotranspiration, T_{avg} is average daily temperature ($^{\circ}C$) defined as the
140 average of the mean daily maximum and mean daily minimum temperature, TD ($^{\circ}C$) is the
141 temperature range computed as the difference between mean daily maximum and mean daily
142 minimum temperature, and RA is extraterrestrial radiation expressed in $[MJm^{-2}d^{-1}]$.

143 Hargreaves method

$$144 \quad ET_o = 0.0023 \times 0.408 \times RA \times (T_{avg} + 17.8) \times TD^{0.5} \quad (7)$$

145 Where, ET_o is reference evapotranspiration, T_{avg} is average daily temperature ($^{\circ}C$) defined as the
146 average of the mean daily maximum and mean daily minimum temperature, TD ($^{\circ}C$) is the
147 temperature range computed as the difference between mean daily maximum and mean daily
148 minimum temperature, and RA is extraterrestrial radiation expressed in $(MJm^{-2}d^{-1})$.

149 For computing the parameter extraterrestrial radiation (RA) is shown in the equation (8).



$$150 \quad RA = \frac{24(60)}{\pi} \times G_{sc} \times d_r \times [w_s \sin(\varphi) \sin(\delta) + \cos(\varphi) \cos(\delta) \sin(w_s)] \quad (8)$$

151 Where, RA is extraterrestrial radiation [$\text{MJm}^{-2}\text{d}^{-1}$], d_r is the inverse relative distance Earth-Sun,
152 G_{sc} is solar constant equals to $0.0820 \text{ MJm}^{-2}\text{min}^{-1}$, w_s is sunset hour angle (rad), δ is solar
153 declination (rad) and φ is latitude (rad).

154 *Determination of Seasonality factor parameter*

155 The seasonality factor z parameter varies depending upon the local precipitation patterns such as
156 the hydrological characteristics of the area, its rainfall intensity and topography. According to the
157 water yield model InVEST (Tallis et al. 2010), the parameter z can be computed in three different
158 ways. First method is suggested by Donohue *et al.* (2012), that the parameter z can be expressed
159 as the one fifth of the number of rain events per year. Second method is suggested by Xu *et al.*
160 (2013), which relates $\omega(x)$ with latitude, NDVI (Normalized Difference Vegetation Index), Area,
161 etc. Third method experiments with various selections of w (one value of w for the entire study
162 region) till there is a good match between observed and computed water yield. Unfortunately, this
163 method is not suited to a pixel based analysis as the number of pixels will be extremely large
164 making the method to be computationally intensive.

165 *2.1.2 Lumped Zhang model*

166 In this model all the mean values of the parameters are used as an input to compute the average
167 value of the water yield for the whole watershed. In this model the averaged actual transpiration,
168 potential evapotranspiration, w , precipitation is used as described by Zhang *et al.* (2004)

169 **3. STUDY AREA**



170 In India, the Ganges ranks amongst the world's top 20 rivers in regards to the flow discharge. The
171 River Ganga is segregated into three zones, viz., Upper Ganga basin, Middle Ganga basin and
172 Lower Ganga basin. The area for the study, i.e., Upper Ganga river basin is situated in the Northern
173 part of India which encompasses an area of around 22,292.1 km². The altitude of the study area
174 varies from 7512 m in the Himalayan terrains to 275 m in the plains. Approximately 433 km² of
175 the entire region of the basin is under glacier landscape and 288 km² is under fluvial landscape.
176 The river basin of Ganga is located in the state of Uttarakhand, India within the geographical
177 coordinates 30° 38' - 31° 24' N latitude and 78° 29' - 80° 22' E longitude with an area of 22,292.1
178 km² upto Haridwar. About 60% of the basin is utilized for agricultural, 20% of the basin is under
179 the forest area, majorly in the upper mountainous region, and nearly 2% of the basin is permanently
180 covered with snow in the mountain peaks. Most predominant soil groups found in the region are
181 sand, clay, loam and their compositions. Due to favorable agricultural conditions majority of the
182 population practices agriculture and horticulture. However, a large portion of the total population
183 lives in cities along Ganga river. In the Upper Ganga river basin, the average annual rainfall varies
184 from 550 to 2500 mm (Bharati et al. 2011) and a major part of the rains is due to the south-westerly
185 monsoon that prevails from July to late September. The geographical location and other
186 information of the study area Upper Ganga river basin are represented in Fig. 1.

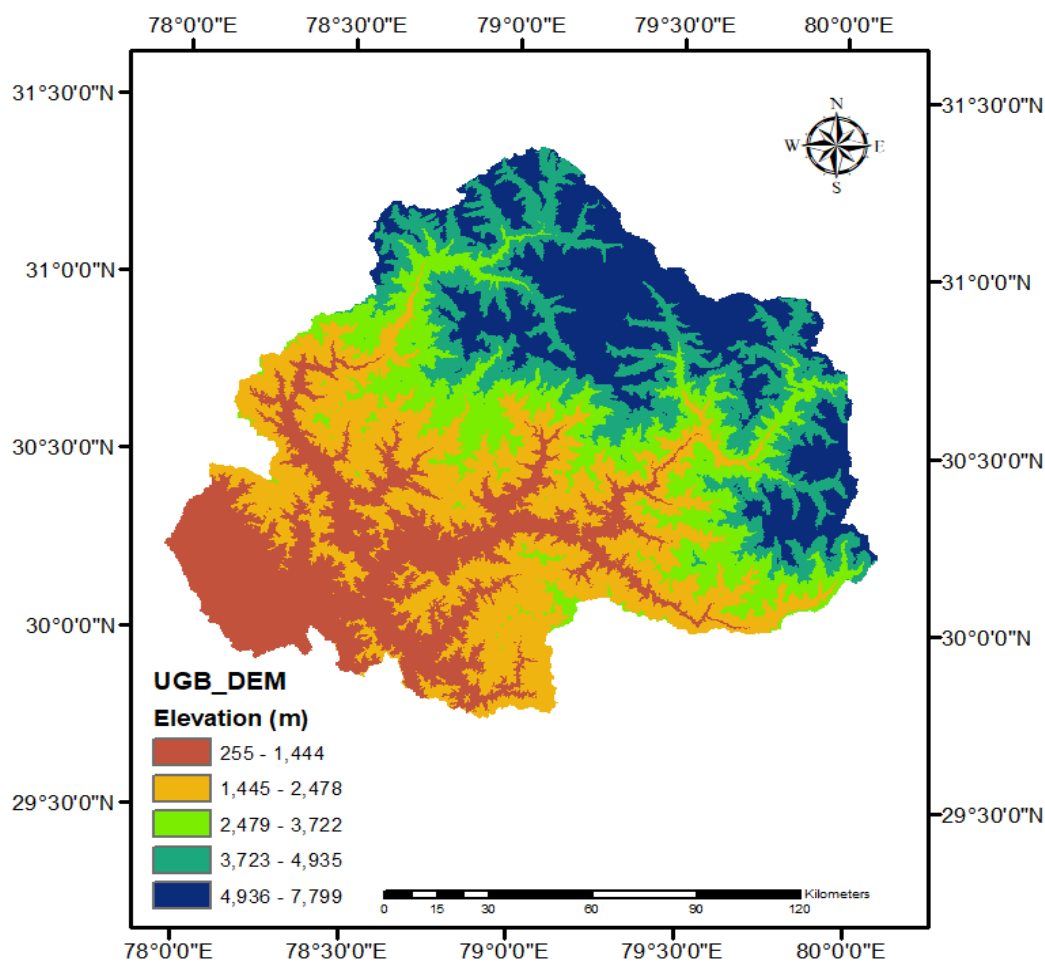


Figure 1. Graphical representation of study area, Upper Ganga basin

4. METHODOLOGY

4.1 Data

4.1.1 Precipitation and Temperature

The daily data of precipitation and temperature for the study area is acquired from India Meteorological Department (IMD) at a grid size of 0.25 degrees and 1 degree, respectively. The study area Upper Ganga basin comes in the latitude ranging from 29.5 degrees to 31.5 degrees and



195 longitude ranging from 77.75 degrees to 80.25 degrees. The data is extracted for all the four years,
196 i.e. 1980, 1990, 2001 and 2015.

197 *4.1.2 Soil Map*

198 Spatial Data of soil is collected from National Bureau of soil survey and land use planning
199 (NBSSLUP) at 1:250000. The cell size of this data is 1200m×1200m which is different from that
200 of land use data which has a cell size of 30m×30m. So this data is resampled using ‘resample’ tool
201 in ArcGIS. The attribute table of the vector layer contains fields like soil depth, soil texture,
202 percentage carbon content, drainage, slope, erosion, soil temperature and mineralogy. The relevant
203 feature, i.e. of soil depth and soil texture are converted into the raster image for the Upper ganga
204 basin.

205 *4.1.3 LandUse/Land Cover map*

206 Different sensors are used for obtaining the satellite images for different years. For the year 1980,
207 1990, 2001 and 2015, Landsat 3/4 ETM, Landsat 4 ETM, Landsat 7 and Landsat 8 ETM sensors
208 are used to download the image.

209 These satellite images are different in their grid size and all the satellite data is taken as raw data
210 from USGS. This data is available in form of different bands combinations and different
211 resolutions depending upon the type of sensors. As per the type of sensors, the bands are stacked
212 in ERDAS and a new stacked image is generated. This image is now classified using supervised
213 classification in ERDAS in six different classes, i.e. Forest, Water, Agricultural, Wasteland, Snow
214 and Glacier and Built-up land. Classification of the area is based upon their similar response under
215 different bands. Each class is then recognized with the help of ground truth and high resolution
216 satellite images.



238 For all the strategies, other steps involving computation of Extraterrestrial Radiation, Precipitation,
239 Temperature, Reference Evapotranspiration and Potential Evapotranspiration are briefly described
240 as follows:

241 4.2.1 Extraterrestrial Radiation $RA(x)$

242 The value of this parameter is computed at a monthly interval in a raster format for different pixels
243 for each month using equation (8).

244 4.2.2 Precipitation; $P(x)$

245 The data is obtained from IMD at grid size 0.25 degree for the study area and has been interpreted
246 and converted to raster format by using IWD interpolation technique for obtaining the values for
247 all pixels at a resolution equal to the resolution of the landsat satellite image for the study area.

248 4.2.3 Temperature $T_{avg}(x)$ and $TD(x)$

249 The temperature data is obtained from IMD at grid size 1 degree for the study area and has been
250 interpreted and converted to raster format by using IWD interpolation technique for obtaining the
251 values for all pixels at a resolution equal to the resolution of the landsat satellite image for the
252 study area. Subsequently, the mean monthly value (T_{avg}) and the difference between mean daily
253 maximum and mean daily minimum (TD) is obtained.

254 4.2.4 Reference Evapotranspiration (ET_o)

255 Modified Hargreaves method is applied for obtaining the values of reference evapotranspiration at
256 each pixel for the study area for each month (Droogers et al. 2002). It is calculated based on the
257 evapotranspiration of grass of the study area. In this method, the inputs are R_a , precipitation, T_{avg}
258 and TD. Some of the months, i.e. July 1980, July 1990, August 1990, June 2001, July 2001, August



259 2001, June 2015, July 2015 and August 2015 showed the negative values of reference
 260 evapotranspiration by applying Modified Hargreaves method. Thus, for the above months the
 261 Hargreaves method, as previously recommended by (Droogers et al. 2002), is applied for obtaining
 262 the positive values for the reference evapotranspiration.

263 Thus, all the mean values for the month are added up to get the mean yearly values for the year
 264 1980, 1990, 2001 and 2015.

265 *4.2.5 Potential Evapotranspiration PET (x)*

266 The yearly values obtained for the reference evapotranspiration have been multiplied by the
 267 vegetation evapotranspiration coefficient (K_c) which varies with the LULC characteristics as
 268 expressed in equation (3). The value of the vegetation evapotranspiration coefficient is taken from
 269 Allen *et al.* (1998). The Table 1. shows the values taken for the coefficient of various classes of
 270 landuse/landcover.

271 **Table 1.** Value of K_c corresponding to LandUse/LandCover classes

S.No.	LandUse/LandCover	Percentage cover (1980)	Percentage cover (1990)	Percentage cover (2001)	Percentage cover (2015)	K_c
1	Forest	17.84	16.32	15.78	15.19	1
2	Water	21.87	21.27	19.47	17.65	1
3	Wastelands	51.1	52.36	54.18	55.46	0.2
4	Built-up Area	2.07	2.14	2.27	2.49	0.4
5	Agricultural	3.67	4.04	3.76	4.22	0.75
6	Snow and Glacier	3.45	3.87	4.54	4.99	2



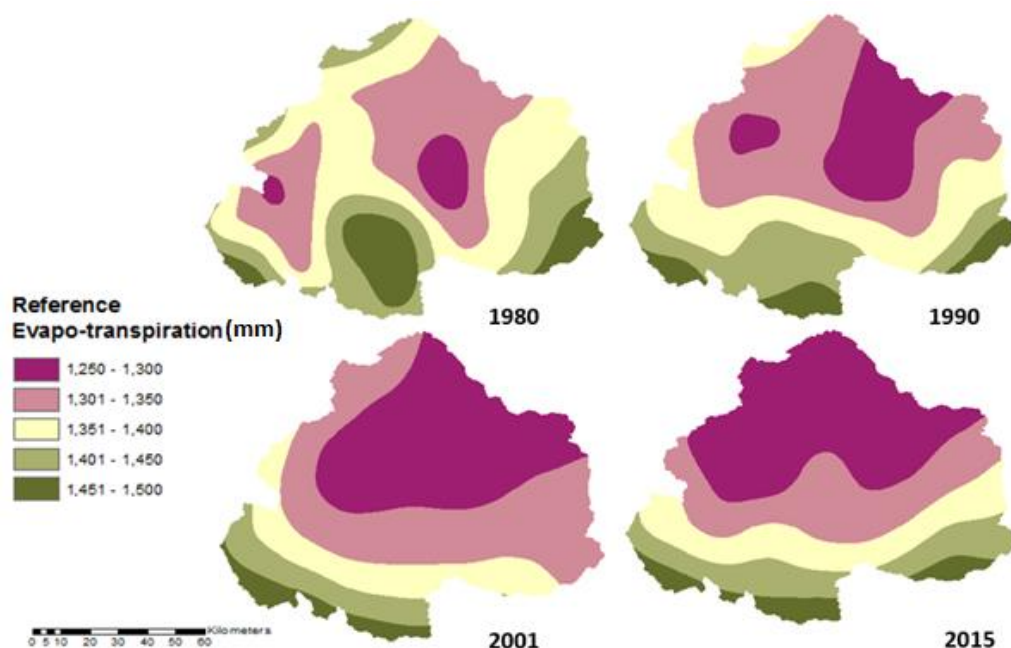
272 In this study, K_c is taken same for all the four years from Table. 1 and is used to obtain potential
273 evapotranspiration which is subsequently used to obtain the yearly potential evapotranspiration at
274 each pixel of the study area.

275 **5. RESULTS**

276 **5.1 Reference Evapotranspiration; $ET_o(x)$**

277 Reference Evapotranspiration is computed for the upper Ganga Basin using a high-resolution
278 monthly climate dataset. Modified Hargreaves method is applied for obtaining the values of
279 reference evapotranspiration at each pixel for the study area for each month (Droogers et al. 2002).
280 The reference evapotranspiration is a function of R_a , precipitation, T_{avg} and TD which are already
281 computed pixel wise for each month for the year 1980, 1990, 2001 and 2015.

282 Some of the months i.e. July 1980, July 1990, August 1990, June 2001, July 2001, August 2001,
283 June 2015, July 2015 and August 2015 showed the negative values of reference evapotranspiration
284 by applying Modified Hargreaves method. Thus for the above months, the Hargreaves method is
285 applied for obtaining the positive results. Hence, all the mean values for the months are added up
286 to get the mean yearly values of evapotranspiration for the years 1980, 1990, 2001 and 2015, as
287 represented in Fig 2.

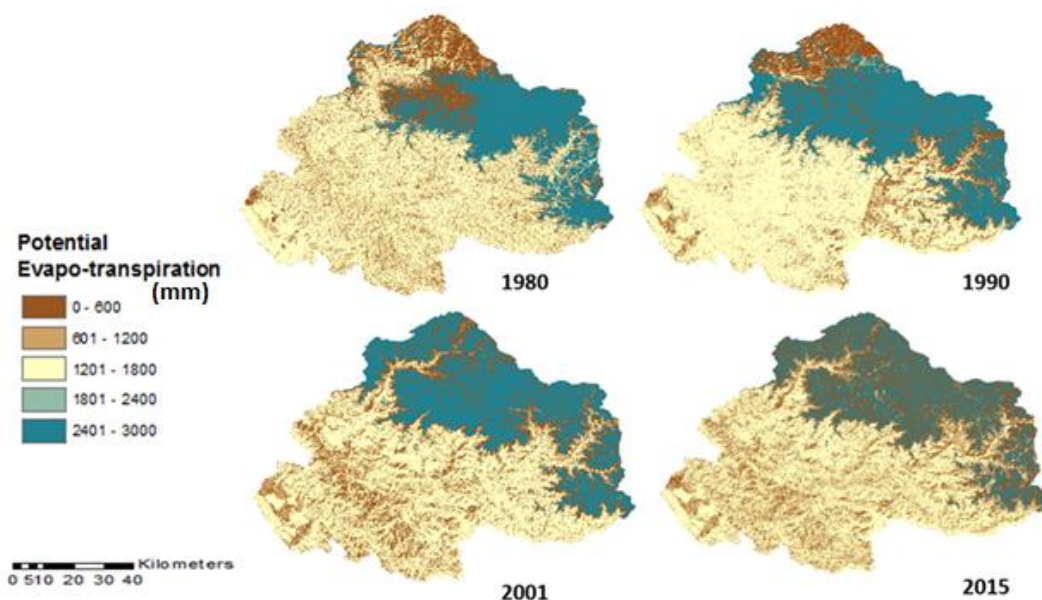


288

289 **Figure 2.** Reference Evapotranspiration (mm) of Upper Ganga Basin for the years 1980, 1990,
290 2001 and 2015.

291 **5.2 Potential Evapotranspiration; $PET(x)$**

292 The yearly values obtained for the reference evapotranspiration is multiplied by the vegetation
293 evapotranspiration coefficient (K_c) which varies with the Land Use Land Cover characteristics, as
294 expressed in equation (3). The value of the vegetation evapotranspiration coefficient is taken from
295 Allen et al. (1998). The values of the vegetation evapotranspiration coefficient are taken from the
296 Table 1. Thus, the potential evapotranspiration is computed for Upper Ganga Basin for the years
297 1980, 1990, 2001 and 2015 as represented in Fig. 3.



298

299 **Figure 3.** Potential Evapotranspiration (mm) of Upper Ganga Basin for the years 1980, 1990, 2001
300 and 2015.

301 **5.3 Water Yield; $Y(x)$**

302 As mentioned in the methodology, the water yield for the Upper Ganga basin are computed using
303 various strategies A, B, C, D and E:

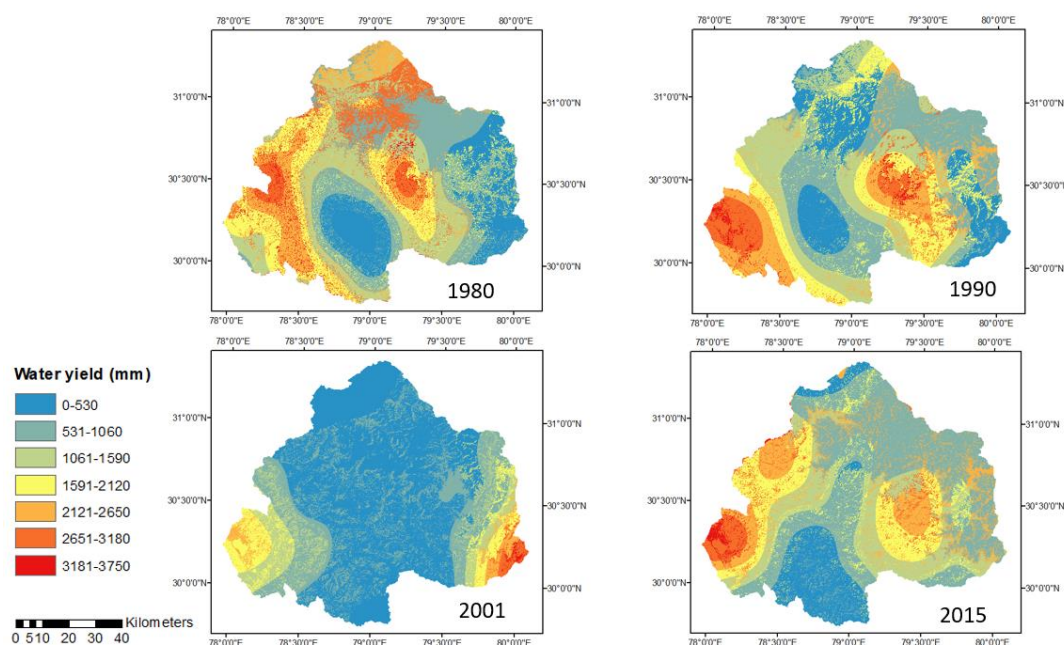
304 ***Strategy A: By computing water yield from Lumped Zhang Model***

305 Here, the mean values of all the input parameters are considered and the water yield is computed
306 for the Upper Ganga basin for the years 1980, 1990, 2001 and 2015 and is obtained as 658.52 mm,
307 925.68 mm, 603.71 mm and 1194.25 mm, respectively.

308 ***Strategy B: Water yield obtained by taking the single weighted mean value of parameter “w”***
309 ***from Xu et al. (2013) for Large basins.***



310 By considering the single value of the parameter “w” for the whole basin the water yield is
311 computed for Upper Ganga basin (equation 9). The weighted mean value for the parameter “w”
312 for the years 1980, 1990, 2001 and 2015 are obtained as 1.507, 1.541, 1.403 and 1.507 respectively.
313 The spatial distribution of water yield for the Upper Ganga basin for the years are represented in
314 Fig. 4. The mean values of water yield for the years 1980, 1990, 2001 and 2015 are 755.65 mm,
315 959.48 mm, 742.39 mm and 1131.42 mm respectively.



316

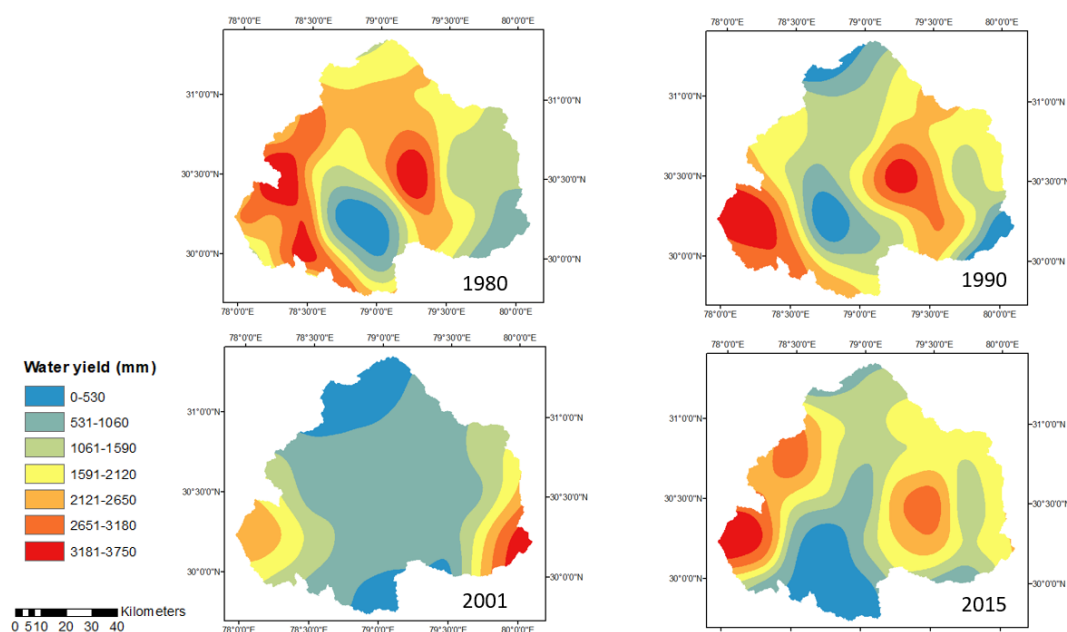
317 **Figure 4.** Water yield obtained by taking the single weighted mean value of parameter “w” from
318 Xu et al. (2013) for large basins.

319 *Strategy C: Water yield obtained by taking the single weighted mean value of parameter “w”*
320 *from Xu et al. (2013) for global model.*

321 By considering the single value of the parameter “w” for the whole basin the water yield is
322 computed for Upper Ganga basin (equation 10). The weighted mean value for the parameter “w”



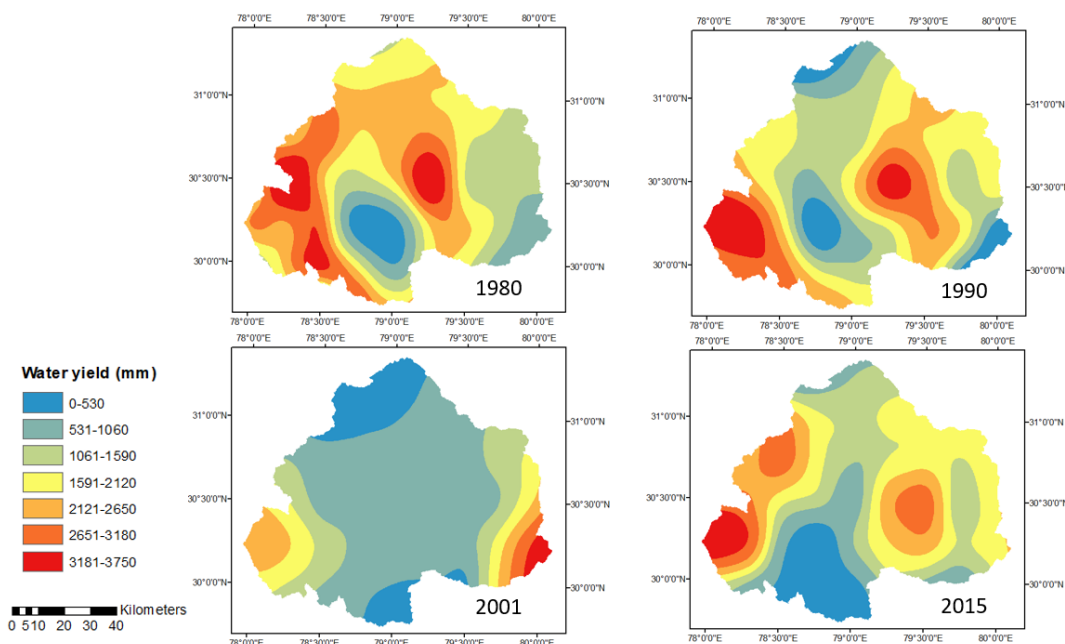
323 for the years 1980, 1990, 2001 and 2015 are obtained as (-0.967), (-0.955), (-1.010) and (-0.968)
324 respectively. The spatial distribution of water yield for the Upper Ganga basin for the years are
325 represented in Fig. 5. The mean values of water yield for the years 1980, 1990, 2001 and 2015 are
326 1239.92 mm, 1549.46 mm, 1149.93 mm and 1754.59 mm respectively.



327
328 **Figure 5.** Water yield obtained by taking the single weighted mean value of parameter “w” from
329 Xu et al. (2013) for global model.

330 *Strategy D: Water yield obtained by computing pixel wise value of parameter “w” from Xu et*
331 *al. (2013)*

332 The values of parameter “w” is computed at pixel level. The water yield computed for the years
333 1980, 1990, 2001 and 2015 for the Upper Ganga Basin are represented in Fig. 6. The mean values
334 of water yield for the years 1980, 1990, 2001 and 2015 are 1240.02 mm, 1549.44 mm, 1149.89
335 mm and 1754.62 mm respectively.

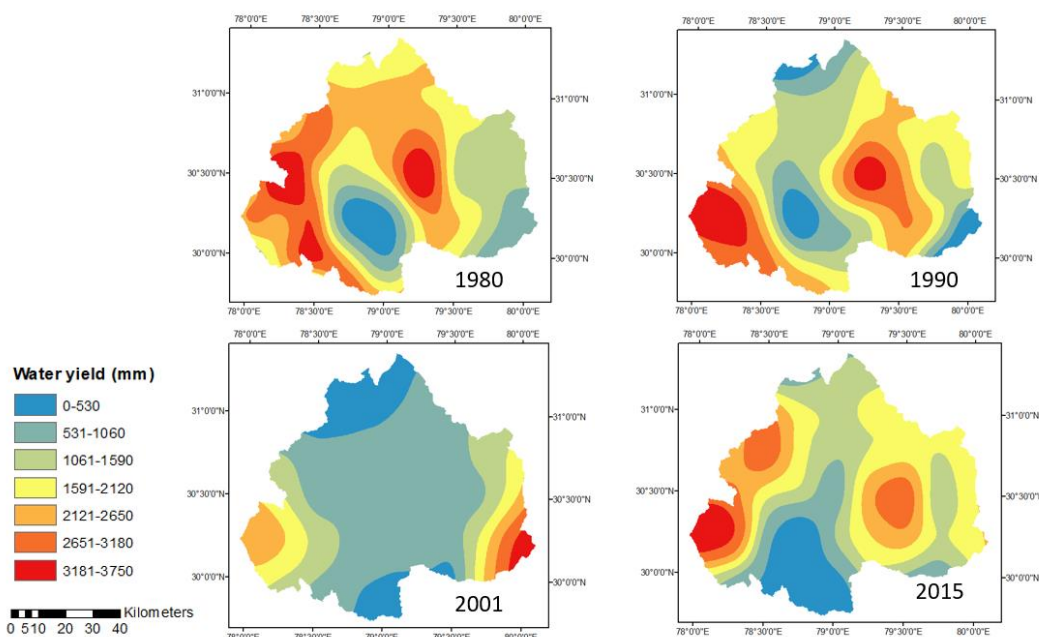


336

337 **Figure 6.** Water yield obtained by computing pixel wise value of parameter “w” from Xu et al.
338 (2013)

339 *Strategy E: Water yield obtained by computing pixel wise value of parameter “w” from Donohue*
340 *et al. (2012)*

341 The equation (4), represents the parameter “w” which is the function of the parameters z, AWC
342 and P. Thus, the water yield is computed for Upper Ganga Basin for the years are shown in Fig. 7.
343 The mean values of water yield for the years 1980, 1990, 2001 and 2015 are 1241.09 mm, 1552.38
344 mm, 1153.95 mm and 1753.53 mm respectively.



345

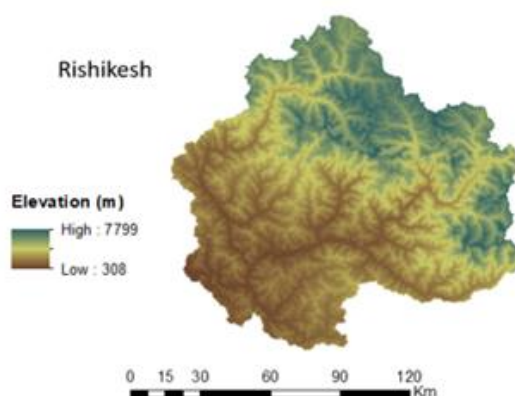
346 **Figure 7.** Water yield obtained by computing pixel wise value of parameter “w” from Donohue *et*
347 *al.* (2012)

348 **5.2 Validation of results in sub-basin Rishikesh of Upper Ganga Basin.**

349 The validation of the yields obtained from various proposed strategies are performed for Rishikesh
350 (Fig. 8), a sub-basins of Upper Ganga basin. As the data of the study area is classified and thus,
351 the representation of complete data is forbidden. The discharge data of the basin is obtained from
352 Irrigation department, Uttarakhand. The surface runoff data is extracted from the snow melting
353 data from the discharge data as the snow melting contributes about 32 percent in study area as
354 suggested by Maurya *et al.* (2011). A comprehensive work on water balance of Upper Ganga Basin
355 has been discussed by Jain *et al.* (2017), with reference to Table 4., in Jain *et al.* (2017). For a
356 Precipitation value of 1236.1 mm, Ground water flow of 293.92 mm and snow melt 73.84 mm. It
357 is apprehended that Ground water flow and snow melt equals to 367.76 mm which is



358 approximately equals to 29.75 percent of Precipitation. Indirectly, this percentage contribution is
 359 also supported by the value reported by Maurya et al. (2011). Thus, the water yield has been
 360 validated for different years by various proposed strategies as shown in Table 2.



361

362 **Figure 8.** Graphical representation of sub-basin Rishikesh

363 **Table 2.** Observed vs computed water yield by various proposed strategies for Rishikesh sub-
 364 basin.

Strategies	1980	1990	2001	2015
Observed discharge (mm)	1831.31	2422.43	2187.22	2835.81
Observed (mm) (after reducing approx. 32% snow melting contribution)	1245.29	1647.25	1487.31	1928.35
Water Yield_Strategy A (mm)	652.47	914.35	598.25	1189.72
Water Yield_Strategy B (mm)	745.38	917.77	697.75	1092.17
Water Yield_Strategy C (mm)	1229.90	1506.82	1102.62	1718.17
Water Yield_Strategy D (mm)	1229.99	1506.74	1102.61	1718.18



Water Yield_Strategy E (mm)	1230.77	1508.88	1106.86	1720.16
-----------------------------	---------	---------	---------	---------

365

366 6. Discussion

367 The study aimed to apply the InVEST water yield model, a tool that is gaining interest in ecosystem
368 services community for Upper Ganga Basin, having the variability in the topography and
369 consisting of hilly areas, plain areas and the regions which are totally covered with snow. The
370 InVEST model is based upon Budyko theory which requires low amount of data and low level of
371 expertise, thus making it acceptable world-wide. Monthly precipitation, monthly average value of
372 temperature, monthly value of difference of mean daily maximum and mean daily minimum and
373 extraterrestrial radiation parameters are computed for the Upper Ganga Basin for each month of
374 all the four years i.e. 1980, 1990, 2001 and 2015 and converted into the raster format for the further
375 analysis. The monthly reference evapotranspiration is thus computed using input parameters in the
376 GIS environment by applying the modified Hargreaves equation for all the months except some
377 months where the modified Hargreaves equation shows the negative results for the reference
378 evapotranspiration value. For those months Hargreaves method is applied to obtain the positive
379 value of reference evapotranspiration as also suggested by Goyal et al. (2017). Reference
380 evapotranspiration when multiplied with K_c gives the potential evapotranspiration. All the monthly
381 values of different years are added up to obtain the yearly value of reference evapotranspiration.
382 K_c is the function of Land Use Land Cover, thus supervised classification is done to prepare the
383 raster Land Use Land Cover map for the Upper Ganga Basin. Thus, the yearly value of potential
384 evapotranspiration is obtained for the study area for the years 1980, 1990, 2001 and 2015.

385 The paper focuses on all the methodologies discussed in the paper and is applied on the Upper
386 Ganga basin. Thus, water yield is computed both from InVEST model as well as Lumped Zhang



387 model. The value of the parameter “w” are computed in four ways, i.e. mean single value obtained
388 from Xu et al. (2013) for large basins and global model, pixel wise value of parameter “w” from
389 Xu et al. (2013) and pixel wise value of parameter “w” from Donohue et al. (2012).

390 The purpose to introduce the value of parameter “w” at pixel level so that it does not seem logical
391 to compute a single value of parameter “w” for such a large basin. Thus, two pixel wise values of
392 parameter “w” is computed for the Upper Ganga basin for years 1980, 1990, 2001 and 2015 by
393 considering two approaches from Xu et al. (2013) and Donohue et al. (2012). Also, the water yield
394 is computed from Lumped Zhang model which works on the approach of considering mean values
395 of all the parameters indulged in the computations of water yield. Thus, in five ways water yield
396 are computed for the Upper Ganga basin for the years 1980, 1990, 2001 and 2015.

397 For site Rishikesh, the contributing area to water yield is extracted from the Upper Ganga basin
398 and the discharge data is taken from the irrigation department, Uttarakhand to compare the results.
399 The surface runoff data is extracted from the snow melting data from the discharge data as the
400 snow melting contributes about 32 percent in study area as suggested by Maurya et al. (2011).
401 Using this fact, the observed yield is compared with the computed water yield based on different
402 proposed strategies for the years 1980, 1990, 2001 and 2015 represented in Table 2.

403 The results obtained from Donohue et al. (2012) and Xu et al. (2013) computed at pixel level
404 (Strategy C, Strategy D and Strategy E), thus represents better performance than other and are in
405 good agreement with the observed data. It is clear that in order to do hydrological processing for
406 any watershed, pixel wise classification and computation is necessary.



407 Hence, it is recommended, that for such a large basin there is a strong need to compute all the
408 parameters involved in the computations of water yield at pixel level scale rather than adopting
409 the mean values for entire watershed.

410 **7. Summary and Conclusions**

411 The study aimed to apply the InVEST annual water yield model, a tool that is gaining interest in
412 the ecosystem services community. While such simple models with low requirements for data and
413 level of expertise are needed for practical applications use of such model with a single
414 representative value for the entire basin does not provide good estimates of water yield. On the
415 other hand, performing pixel scale computation of water yield indicates a better performance and
416 results obtained show better agreement with the observed water yield. Regarding the use of
417 parameter “w” global model works better than other representation of “w” available in literature.

418 The water yield is computed in five different ways and results are analyzed with the observed data
419 of sub-basins of Upper Ganga Basin. Earlier, some of the important parameters for the water yield
420 used to be computed at a basin level scale which brings noise in the results. Thus, by considering
421 all the parameters involved in the model at pixel level scale, the results obtained are higher in
422 accuracy.

423 Thus it is inferred that,

- 424 1) Between two approaches used, i.e. considering entire basin and pixel level approach, the
425 pixel level approach is found to provide better results.
- 426 2) In pixel level based computations, results further improved with the use of a parameter
427 “w” based on a global model than regional models of “w” for large basins in Himalayan
428 basin.



429 **Acknowledgement**

430 Authors are thankful to Executive Engineer, Irrigation Department, Uttarakhand, for providing the
431 discharge data for the Rishikesh sub-basin of Upper Ganga Basin.

432 **References**

433 Allen, R. G., Pereira, L. S., Raes, D., and Smith, M. (1998). “Crop evapotranspiration-Guidelines
434 for computing crop water requirements”-FAO Irrigation and drainage paper 56. FAO, Rome,
435 300(9), D05109.

436 Bai, Y., Ouyang, Y., and Pang, J. S. (2012). “Biofuel supply chain design under competitive
437 agricultural land use and feedstock market equilibrium.” *Energy Economics*, 34(5), 1623-1633.

438 Bharati, Luna, Guillaume Lacombe, Pabitra Gurung, Priyantha Jayakody, Chu Thai Hoanh, and
439 Vladimir Smakhtin (2011). *The impacts of water infrastructure and climate change on the*
440 *hydrology of the Upper Ganges River Basin*. Vol. 142. IWMI, 2011.

441 Budyko, M. I. (1974). *Climate and Life*, Academic Press, New York, USA, 1-507.

442 Budyko, M. I., and Ronov, A. B. (1979). “Evolution of chemical composition of the atmosphere
443 during the Phanerozoic.” *Geokhimiya*, (5), 643-653.

444 Burkhard, B., Crossman, N., Nedkov, S., Petz, K., and Alkemade, R. (2013). “*Mapping and*
445 *modelling ecosystem services for science, policy and practice*.1-3.

446 Choudhury, B. (1999). “Evaluation of an empirical equation for annual evaporation using field
447 observations and results from a biophysical model.” *Journal of Hydrology*, 216(1), 99-110.



- 448 Donohue, R. J., Roderick, M. L., and McVicar, T. R. (2012). “Roots, storms and soil pores:
449 Incorporating key ecohydrological processes into Budyko’s hydrological model.” *Journal of*
450 *Hydrology*, 436, 35-50.
- 451 Droogers, P., and Allen, R. G. (2002). “Estimating reference evapotranspiration under inaccurate
452 data conditions.” *Irrigation and drainage systems*, 16(1), 33-45.
- 453 Fu, B. P. (1981). “On the calculation of the evaporation from land surface.” *Sci. Atmos. Sin*, 5(1),
454 23-31.
- 455 Goyal, M. K., and Khan, M. (2017). “Assessment of spatially explicit annual water-balance model
456 for Sutlej River Basin in eastern Himalayas and Tungabhadra River Basin in peninsular India.”
457 *Hydrology Research*, 48(2), 542-558.
- 458 Guswa, A. J., Brauman, K. A., Brown, C., Hamel, P., Keeler, B. L., and Sayre, S. S. (2014).
459 “Ecosystem services: Challenges and opportunities for hydrologic modeling to support decision
460 making.” *Water Resources Research*, 50(5), 4535-4544.
- 461 Hamel, P., and Guswa, A. J. (2014). “Uncertainty analysis of a spatially-explicit annual water-
462 balance model: case study of the Cape Fear catchment, NC.” *Hydrology and Earth System*
463 *Sciences*, 11, 11001-11036.
- 464 Hoyer, R., and Chang, H. (2014). “Assessment of freshwater ecosystem services in the Tualatin
465 and Yamhill basins under climate change and urbanization.” *Applied Geography*, 53, 402-416.
- 466 Jain, S. K., Jain, S. K., Jain, N., and Xu, C. Y. (2017). “Hydrologic modeling of a Himalayan
467 mountain basin by using the SWAT mode.” *Hydrology and Earth System Sciences*,
468 <https://doi.org/10.5194/hess-2017-100>



469 Khatami, S., and Khazaei, B. (2014). “Benefits of GIS Application in Hydrological Modeling: A
470 Brief summary.” *VATTEN–Journal of Water Management and Research*, 70, 41-49.

471 Liston, G. E., and Elder, K. (2006). “A distributed snow-evolution modeling system
472 (SnowModel).” *Journal of Hydrometeorology*, 7(6), 1259-1276.

473 Maurya, A. S., Shah, M., Deshpande, R. D., Bhardwaj, R. M., Prasad, A., and Gupta, S. K. (2011).
474 “Hydrograph separation and precipitation source identification using stable water isotopes and
475 conductivity: River Ganga at Himalayan foothills.” *Hydrological Processes*, 25(10), 1521-1530.

476 McKenzie, N. J., Gallant, J., and Gregory, L. (2003). “Estimating water storage capacities in soil
477 at catchment scales.” *CRC for Catchment Hydrology*.

478 Milly, P. C. D., and Dunne, K. A. (2002). “Macroscale water fluxes 2. Water and energy supply
479 control of their interannual variability.” *Water Resources Research*, 38(10).

480 Nelson, E., Sander, H., Hawthorne, P., Conte, M., Ennaanay, D., Wolny, S., ... and Polasky, S.
481 (2010). “Projecting global land-use change and its effect on ecosystem service provision and
482 biodiversity with simple models.” *PloS one*, 5(12), e14327.

483 Ojha C.S.P., Bhunya P., and Berndtsson R. (2008). *Engineering Hydrology*, 1st Ed., Oxford
484 University Press, UK, 1-459.

485 Sánchez-Canales, M., Benito, A. L., Passuello, A., Terrado, M., Ziv, G., Acuña, V., ... and Elorza,
486 F. J. (2012). “Sensitivity analysis of ecosystem service valuation in a Mediterranean watershed.”
487 *Science of the total environment*, 440, 140-153.

488 Su, C., and Fu, B. (2013). “Evolution of ecosystem services in the Chinese Loess Plateau under
489 climatic and land use changes.” *Global and Planetary Change*, 101, 119-128.



- 490 Tallis, H.T., Ricketts, T., Nelson, E., Ennaanay, D., Wolny, S., Olwero, N., Vigerstol, K.,
491 Pennington, D., Mendoza, G., Aukema, J. and Foster, J., (2010). *InVEST 1.004 beta User's Guide*.
492 The Natural Capital Project.
- 493 Terrado, M., Acuña, V., Ennaanay, D., Tallis, H., and Sabater, S. (2014). "Impact of climate
494 extremes on hydrological ecosystem services in a heavily humanized Mediterranean basin."
495 *Ecological Indicators*, 37, 199-209.
- 496 Wang, D., and Tang, Y. (2014). "A one-parameter Budyko model for water balance captures
497 emergent behavior in darwinian hydrologic models." *Geophysical Research Letters*, 41(13), 4569-
498 4577.
- 499 Xu, X., Liu, W., Scanlon, B. R., Zhang, L., and Pan, M. (2013). "Local and global factors
500 controlling water-energy balances within the Budyko framework." *Geophysical Research Letters*,
501 40(23), 6123-6129.
- 502 Zhang, L., Dawes, W. R., and Walker, G. R. (2001). "Response of mean annual evapotranspiration
503 to vegetation changes at catchment scale." *Water resources research*, 37(3), 701-708.
- 504 Zhang, L., Hickel, K., Dawes, W. R., Chiew, F. H., Western, A. W., and Briggs, P. R. (2004). "A
505 rational function approach for estimating mean annual evapotranspiration." *Water Resources*
506 *Research*, 40(2).
- 507 Zhou, X., Zhang, Y., Wang, Y., Zhang, H., Vaze, J., Zhang, L., ... and Zhou, Y. (2012).
508 "Benchmarking global land surface models against the observed mean annual runoff from 150
509 large basins." *Journal of Hydrology*, 470, 269-279.